

## STEM-in-SEM Imaging and Diffraction with Extremely Beam Sensitive Ultrathin Zeolites

Jason Holm

NIST, Boulder, Colorado, United States

Zeolites are used in numerous applications [1]. As a material class, zeolites are highly susceptible to electron beam damage: knock-on damage prevails at high beam energies and radiolytic damage at low energies [2]. Even at conventional scanning electron microscope (SEM) energies structural damage occurs rapidly, and what were initially strong diffraction spots fade quickly making imaging and diffraction studies challenging. Here, a four-dimensional scanning transmission electron microscopy in a scanning electron microscope (4D STEM-in-SEM) approach is used as a low dose technique to demonstrate that despite the inevitable beam damage, meaningful images and crystallographic information can be obtained from ultrathin zeolite nanosheets [3] at beam energies typical of an SEM (i.e.,  $\leq 30$  keV).

The 4D STEM-in-SEM setup used here is described in detail elsewhere [4]. Briefly, a scintillator, mirror assembly, and CCD camera are used to image electrons forward scattered through the sample in a Zeiss Gemini 300 SEM [5]. LabVIEW is used to synchronize the electron beam and camera, and MATLAB is used for offline 4D dataset analyses. Low dose imaging is implemented via the short dwell times (i.e.,  $\leq 10$  ms) at each beam raster point.

Figure 1 shows 30 keV (680 pA beam current) images and diffraction patterns (DPs) from a 4D dataset obtained using 10 ms dwell time at each beam raster point. Fig. 1a shows the average of all 160,000 DPs comprising the dataset, while Fig. 2b shows an annular dark-field (ADF) image obtained using a digital annular aperture (i.e., the region between the green circles in Fig. 1a encircling only (101) and (200) reflections). Although the average DP in is rather nondescript, the ADF image in Fig. 1b is crisp, with intensities quantized according to sample thickness. Fig. 1c is a single DP obtained from two overlapping sheets at the red cross in Fig. 2b, showing that distinct spots can be observed using a short dwell time. Fig. 1d is a dark-field image based on (501) reflections from one of the sheets (Fig. 1c, red circles), demonstrating how a virtual aperture can be used to highlight sheets with specific orientation.

A slightly different use of the experimental setup is shown in Figure 2. Here, 7.5 keV electrons and a 7.5  $\mu\text{m}$  final lens aperture were used in an underfocused condition (i.e., 50 mm working distance) to obtain low beam current (19.5 pA) and approximately parallel illumination. Rather than recording a full 4D dataset, the beam was rastered over a small region of the sample (11.4  $\mu\text{m} \times 8.6 \mu\text{m}$ , 1024 px  $\times$  768 px image, 89 ms cycle time) while a long exposure image (60 s) was recorded. Fig. 2a shows the resulting ring diffraction pattern where distinct rings are visible and the red arcs indicate software-identified reflections. Fig. 2b shows the azimuthally-integrated intensity profile with many distinct peaks. Figure 2c shows a convergent beam DP obtained at 20 keV. Combined, Fig. 2b and 2c enable assignment of every peak/reflection in the figure. Moreover, the peak positions in Fig. 2b agree remarkably well with unit cell dimensions obtained from X-ray diffraction studies [3]. Note that Fig. 2c contains information beyond that in Fig. 2b. (The inset green circle shows the range of scattering information obtained at 7.5 keV.) For example, part of the (10 0 0) ring is visible in 2b, but the (16 0 0) reflections are discernible in 2c.

The utility of using a 4D STEM-in-SEM setup for examining beam sensitive zeolite sheets has been demonstrated. A major benefit the approach is that once a 4D dataset has been obtained, it can be revisited numerous times in various ways including, for example, the use of higher order reflections to highlight sheets with specific orientation, and using multiple reflections to improve the signal-to-noise ratio in real-space images. Another benefit is that by decoupling the camera from the scan coils and rastering the beam over a selected region of the sample, weak high order reflections can be observed by using longer exposures.

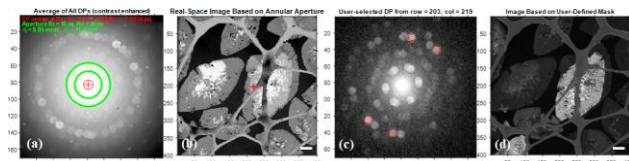


**Figure 1.** (a) Average of all  $400 \times 400$  DPs in a 30 keV dataset. Green circles indicate the digital aperture used for the annular dark-field image in (b), where the red cross indicates the source location of (c) the DPs from two overlapping sheets. The red circles indicate the digital aperture (i.e., the (501) reflections from one sheet) used for (d) a dark-field image highlighting one of the overlapping sheets. DPs are labeled in camera pixel coordinates, and real-space images in beam raster position coordinates to indicate the range of 4D dataset coordinates. Scale bars are 400 nm.

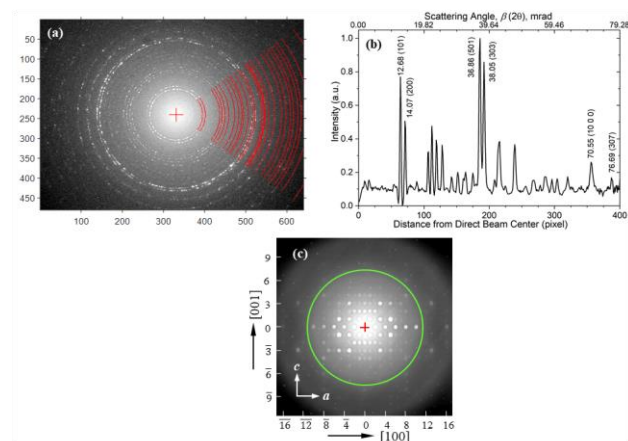


**Figure 2.** (a) A ring DP obtained at 7.5 keV with  $7.5 \mu\text{m}$  final lens aperture, 50 mm working distance (underfocused beam), and long camera length for approximately parallel illumination. Red cross indicates the center of the direct beam, axes are in camera pixel coordinates, and the red arcs show software-identified reflections/rings. (b) The azimuthally integrated (background subtracted) intensity profile of (a). Select peaks are labeled with scattering angle,  $\beta$ , and reflection (hkl). (c) A 20 keV convergent beam DP used to confirm ring identification. Axes are in (hkl) coordinates.

## References

- [1] Kumar, P., et al. *Nature Materials* 2020 (19) 449-449.
- [2] Ugurlu, O., et al., *Phys. Rev. B* 2011 (83) 113408.
- [3] Jeon, M. Y., et al. *Nature* 2017 (543) 690-694.
- [4] Caplins, B. W., et al., *Ultramicroscopy* 2020 (291) 113137.
- [5] Trade names and company products identified in the text do not imply recommendation or endorsement by NIST, nor do they imply that the products are best suited for the purpose.